Investigating the properties of interfacial layers in planar Schottky contacts on hydrogen-terminated diamond through DC/small-signal characterization and radial line small-signal modelling

Supplemental Material

Mathematical derivation of the distributed radial line input admittance

We refer in the following to the equivalent circuit in Fig. 4 of the manuscript.

The per-unit-length parameters (p.u.l) of the radial line can be derived by considering a circular section of length dr with radius r, whose parallel capacitance and conductance model the gate/IL/channel cross section, whereas the series resistance describes hole transport across the channel:

$$\begin{aligned} \mathrm{d}C &= C_{\mathrm{GC}} 2\pi r \mathrm{d}r \\ \mathrm{d}G &= G_{\mathrm{d}} 2\pi r \mathrm{d}r \\ \mathrm{d}R &= R_{\mathrm{ch}} \frac{\mathrm{d}r}{2\pi r} \end{aligned} \tag{1}$$

where, with reference to Fig. 4, the gate-channel capacitance $C_{\mathrm{GC}}(V)$ is defined as

$$C_{\mathrm{GC}}(V) = \frac{C_{\mathrm{IL}} C_{\mathrm{ch}}}{C_{\mathrm{IL}} + C_{\mathrm{ch}}}. \tag{2}$$

The parameters C_{IL} and $C_{\mathrm{ch}}(V)$ are the per-unit-area IL and channel capacitance, respectively. In Eq.(1), G_{d} is the per-unit-area conductance accounting for the gate-channel leakage current. Finally, $R_{\mathrm{ch}} = 1/(q\mu_h p_s)$ is the equivalent channel sheet resistance, where μ_h and p_s are the 2DHG mobility and sheet density, respectively. The 2DHG concentration is evaluated self-consistently with the gate-channel capacitance of the circular section as

$$p_{\mathrm{s}}(V_{\mathrm{G}}) = -\frac{1}{q} \int_{V_{\mathrm{G0}}}^{V_{\mathrm{G}}} C_{\mathrm{GC}}(V) \, \mathrm{d}V \tag{3}$$

where V_{G0} is a bias point in the off state, such that $p_{\mathrm{s}}(V_{\mathrm{G0}}) = 0$.

Applying the Kirchhoff's voltage and current laws to a line section of radial length dr located in r, the line equations result as

$$\begin{aligned} \frac{dV}{dr} &= -\frac{R_{\mathrm{ch}}}{2\pi r} I \\ \frac{dI}{dr} &= -Y_{\mathrm{p}} 2\pi r V \end{aligned} \tag{4}$$

with $Y_\mathrm{p} = G_\mathrm{d} + j\omega C_\mathrm{GC}$. Differentiating, substituting and exploiting the variable change $x = \sqrt{Y_\mathrm{p} R_\mathrm{ch}}\, r$, we have for the line voltage

$$x^2 \frac{\mathrm{d}^2 V}{\mathrm{d}x^2} + x\frac{\mathrm{d}V}{\mathrm{d}x} - x^2 V = 0 \tag{5}$$

i.e. a zero-order Bessel differential equation, admitting a closed-form solution in terms of modified Bessel functions of the first (I) and second (K) kind. The resulting values for the line current and voltage are, respectively:

$$\begin{aligned} I(r) &= A 2\pi r \sqrt{\frac{Y_\mathrm{p}}{R_\mathrm{ch}}} I_1(kr) + B 2\pi r \sqrt{\frac{Y_\mathrm{p}}{R_\mathrm{ch}}} K_1(kr) \\ V(r) &= A I_0(kr) + B K_0(kr), \end{aligned} \tag{6}$$

where A and B are integration constants, and $k = \sqrt{Y_\mathrm{p} R_\mathrm{ch}}$. The line current is derived from the voltage by differentiation. Finally, considering a line with radius R and applying the boundary conditions $I(r=0) = 0$ and $V(r=R) = V_0$, the line input admittance is calculated as

$$Y_\mathrm{i} = \frac{I(R)}{V(R)} = 2\pi R \sqrt{\frac{Y_\mathrm{p}}{R_\mathrm{ch}}} \frac{I_1(kR)}{I_0(kR)}. \tag{7}$$

The total equivalent impedance of the device is then computed by including the effect of the parasitic access and contact resistances (R_s) as $1/Y_\mathrm{i} + R_\mathrm{s}$.

The analytic model has been validated against 3D physics-based simulations[1], under AC condition, of a planar device with 5 nm thick IL ($\epsilon_r = 9$), carrier mobility of 50 $\mathrm{cm^2V^{-1}s^{-1}}$, and radius of 25 μm. Fig. S1 shows the parallel capacitance and conductance associated with the small-signal admittance $Y_\mathrm{i} = G_\mathrm{i} + j\omega C_\mathrm{i}$ as derived from the physics-based simulation and as predicted by Eq. (7), demonstrating the high accuracy of the analytic distributed model.

As discussed in the manuscript, reducing the gate radius to a few μm will make the dispersive effect of the channel resistance (R_ch in Fig. 4 of the manuscript) negligible, thus allowing the accurate extraction of the physical paramaters by a lumped model that can be derived from the series expansion of Eq. (7) when $kR \to 0$. Truncating the series at the 4th order, one obtains

$$Y_\mathrm{i,lumped} = \pi R^2 Y_\mathrm{p} - \frac{\pi R^4}{8} Y_\mathrm{p}^2 R_\mathrm{ch}. \tag{8}$$

The approximation admits for an interpetation in terms of a lumped equivalent circuit made by the series of the admittance $\pi R^2 Y_\mathrm{p}$ and the resistance $R_\mathrm{ch}/8/\pi$, as can be demonstrated from the series expansion of the input impedance $1/Y_\mathrm{i}$. Thus, in the lumped limit,

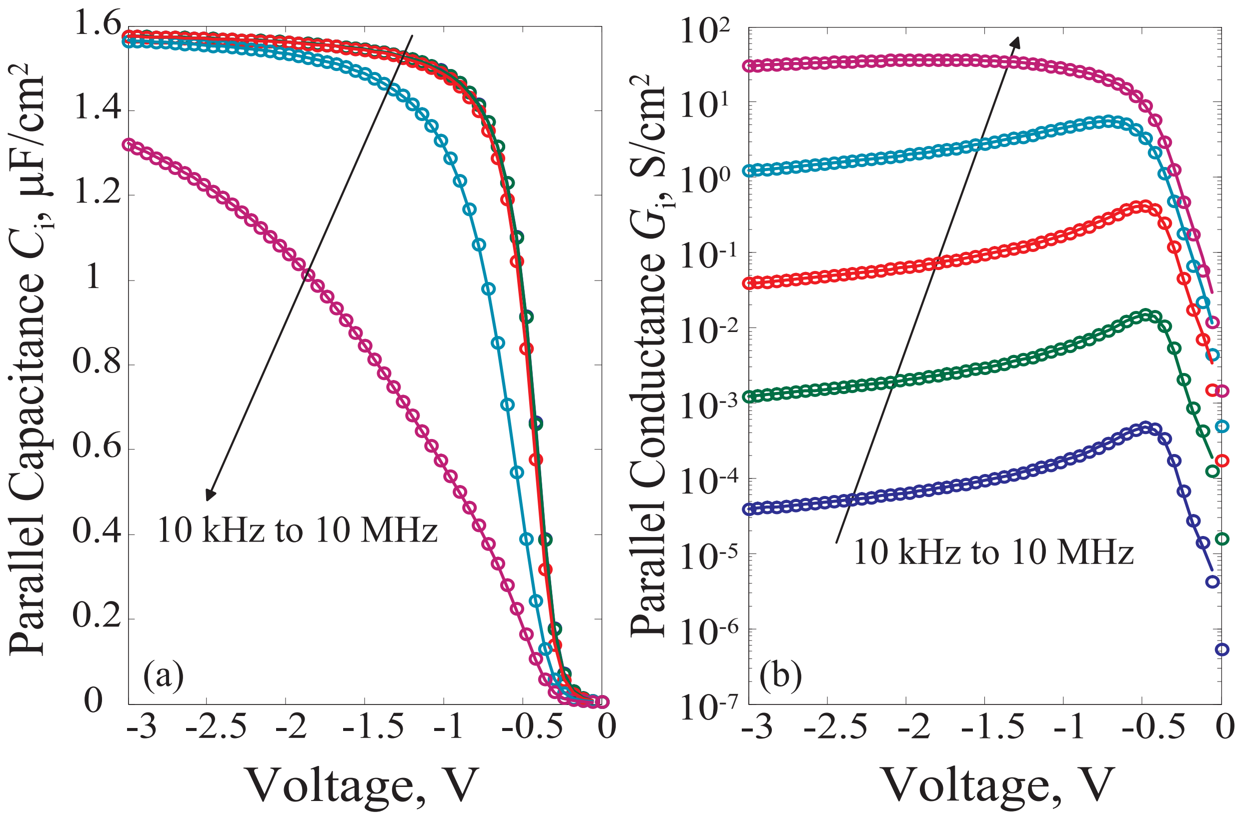

FIG. S1. C_{i}/V (a) and G_{i}/V (b) curves at various frequencies of a large area planar device as predicted by physics-based simulations (symbols) and by the analytical distributed model in Eq. (7) (solid lines). Frequency points are logarithmically equally spaced between 10 kHz and 10 MHz.

the equivalent resistance of the line is the sheet resistance (R_{ch}) corrected by a suitable scale factor ($1/8/\pi$).

REFERENCES

[1] "Sentaurus Device, Synopsys Inc." (2014).